Available online at www.sciencedirect.com
SCIENCE DIRECT®
Journal of Solid State Chemistry 178 (2005) 1145–1156
JOURNAL OF SOLID STATE CHEMISTRY
www.elsevier.com/locate/jssc

The photochromic effect of bismuth vanadate pigments. Part I: Synthesis, characterization and lightfastness of pigment coatings

A. Tücks, H.P. Beck*

Institut für Anorganische und Analytische Chemie und Radiochemie, Universität des Saarlandes, Postfach 151150, D-66041 Saarbrücken, Germany

Received 14 October 2004; accepted 7 November 2004

Abstract

We report on investigations of the photochromic effect of $BiVO_4$ pigments. Emphasis is placed on an approach widely used in industrial color testing. By means of colorimetry ΔE_{ab}^*-values, which measure the perceived color difference, can be calculated from reflectance spectra of non-illuminated and illuminated pigment coatings. Pigments were prepared by either wet-chemical precipitation or solid-state reactions. Depending on the choice of starting compounds, lightfastness was found to vary significantly. Small amounts of impurity phases do not seem to affect photochromism. In contrast, impurities like Fe and Pb cause intense photochromism. The role of Fe is suggested by trace analyses, which (in case of pigments synthesized by precipitation reactions) reveal a correlation between concentration and ΔE_{ab}^*. Indications are found that other effects like pigment–lacquer interactions might also be of importance. Difference reflectance spectra turn out to vary in shape depending on the type and concentration of impurities or dopants. For $BiVO_4$ at least three different mechanisms of photochromism can be assumed.

Keywords: $BiVO_4$; Pigment coatings; Photochromism; Photochromic effect; Colorimetry; Reflectance spectroscopy; Illumination; Trace analysis

1. Introduction

During the last decades, numerous inorganic materials with diverse optical properties, including single crystals as well as polycrystalline powders, have been developed for technical applications. One group of compounds exhibits the remarkable phenomenon of changing its optical characteristics (index of refraction and absorption) under the influence of light. Photorefractive crystals are very interesting and promising materials with respect to data storage (holography), and in this case the modification of optical constants is desired [1]. The opposite is true for coloring materials like inorganic pigments which are designed for the best possible stability against light (lightfastness) and other impacts. In the field of pigment production and characterization, the term photochromism is often applied. By definition, photochromism implies reversible changes in the absorption properties of materials (and thus color changes) due to the influence of radiation. If kept in the dark, illuminated samples return to their initial state (thermal bleaching).[1] Most studies on photochromism of pigments seem to be carried out in industrial laboratories but examples for photochromic substances can be found in the literature, e.g. V_2O_5 [2], MoO_3 [3], WO_3 [4], perovskites [5–7], $PbMoO_4$ [8], and photochromic glasses [9,10], to name the more familiar ones. In some cases, detailed information about light-induced processes on an atomic scale is available (WO_3 is one of the most intensively studied compounds).

Some papers report on different properties of $BiVO_4$ (synthesis [11,12], phase diagrams [13,14], ferroelasticity [15], epr investigations [16]), but to our knowledge no systematic studies on photochromic properties have

*Corresponding author. Fax: +49 681 302 4233.
E-mail address: hp.beck@mx.uni-saarland.de (H.P. Beck).

[1] In contrast to photochromism, the term lightfastness does not imply reversibility and is therefore more general.

0022-4596/$ - see front matter © 2004 Elsevier Inc. All rights reserved.
doi:10.1016/j.jssc.2004.11.025

been published so far. As $BiVO_4$ provides the basis for high-quality yellow pigments, which can be considered as an alternative for CdS or $PbCrO_4$-based pigments, a deeper insight into the mechanism of photochromism and in-depth knowledge of potential factors of influence are desirable.

In this first part, we describe some basic concepts needed to quantitatively describe the extent of photochromism by means of colorimetry, which are suitable to characterize pigment coatings and are widely applied in industrial test procedures. Preparation methods and their influence on phase purity, investigated by powder diffraction and infra-red spectroscopy, are discussed. Results of illumination experiments are presented, and correlations between the extent of photochromism and impurity levels are proposed and tested. Details about the mechanism(s) of photochromism can only be assumed at this stage. The second part[2] will be dedicated to more fundamental studies and involves electron paramagnetic resonance spectroscopy and investigations of interactions between pigment particles and the surrounding medium. Additionally, the behavior of powder samples will be discussed and compared to pigment lacquers.

2. Experimental

2.1. Pigment synthesis and after-treatment

Pigments were synthesized by either wet-chemical precipitation or solid-state reactions using different combinations of educts. In case of the former method, a brief description is given for a typical procedure. Possible modifications primarily include the Bi:V ratio, the choice of pH and the way it is controlled during synthesis.

2.1.1. Wet-chemical precipitation reaction

Alkaline vanadate solutions were added dropwise to acidic solutions of bismuth. Adjusting the pH to either 3.8 or 4.5, the suspension was heated to 90 °C (pH control, see below) or 96 °C. Initially, pH slowly increased, but after about 2 h a quick rise was observed and the pale orange-yellow amorphous precipitate started to transform to a bright yellow crystalline substance. On reaching pH 4.8, either nitric acid was continuously added to keep a constant value of 4.8 for 3 h, or the pH was allowed to develop. In some cases, ammonium nitrate was added to the bismuth solution (passive pH control). The suspension was cooled down to room temperature and the precipitate filtered off, washed with de-ionized water and dried at 130 °C.

[2]Part II: investigations on the photochromic mechanism (to be published).

pH ▶	4.5 ↗ X	3.8 ↗ X	3.8 ↗ X (NH_4^+-buffer)	3.8 ↗ 4.8	Ball-Milling ▼
2 h 500 °C	●●●	●●●	●●●	●	60 min
2 h 500 °C 0.5 h 620°C	○	●	●	●●●	90 min
3 × 10 h 650 °C	●	●	○	○	12 h
▲ Annealing	Bi / V solutions dissolved solids		Bi / V solutions only dissolved solids for doping		◀ Educts

●●● standard procedure ● selected pigments only ○ combination not used

Fig. 1. Survey of synthesis parameters for wet-chemical precipitation reactions (the mechanical treatment on the right corresponds to the thermal treatment given in the same row on the left; educts in the bottom row refer to the first two and last two columns of the different pH programs, respectively).

All pigments were annealed according to at least one of the following schemes: 2 h 500 °C, 2 h 500 °C and 30 min 620 °C, 3 times 10 h 650 °C (the latter includes intermediate grinding, see solid-state reaction). An overview of synthesis parameters is given in Fig. 1.

The preparation of singly doped pigments was achieved by adding soluble compounds of the corresponding dopant to the bismuth or vanadate solution before mixing.

2.1.2. Solid-state reaction

Mixtures of suitable educts[3] (oxides, basic bismuth nitrate, ammonium vanadate; characterized by trace analysis, see Results and discussion) and agate grinding balls were placed in agate grinding bowls under diethyl ether and thoroughly ground utilizing a planetary micro-mill *Pulverisette* 7 (Fritsch). The powders were heated in platinum crucibles 2 or 3 times to 650 °C for 10 h and re-ground before the second and third annealing step.

2.1.3. After-treatment

In order to obtain pigments with good dispersibility, all powders were subjected to wet-milling. In the case of bismuth vanadate, this is mandatory for compounds annealed above approx. 400 °C, which might additionally exhibit undesired color properties due to large particle sizes. 15.0 g pigment, 12.0 g lead-free glass beads and 12.0 g de-ionized water ($\geqslant 18.2\,M\Omega\,cm$) were placed in agate grinding bowls. The duration of grinding was chosen according to the thermal treatment of the corresponding pigment (always 12 h for pigments prepared by solid-state reaction). After ball-milling, the water was removed by vaporization.

[3]Investigations of photochromic materials do not necessarily require high-purity compounds for synthesis. As will become clear later, it is quite helpful to use educts with different distributions of impurities to gain insight into their effects.

2.2. X-ray powder diffraction

The phase purity of all pigments (before and after ball-milling) was controlled by means of X-ray powder diffraction utilizing a D5000 diffractometer (Siemens) with Cu$K\alpha_1$ radiation and a position sensitive detector. In order to detect small amounts of crystalline impurities, an exposure time of 12 h was chosen.

2.3. Infra-red spectroscopy

Infra-red spectra were recorded on a single beam FT-IR spectrometer *Spectrum* 2000 (Perkin–Elmer) equipped with a DRIFT accessory (*The Selector*, 19900 series, Specac). The pigments were mixed with an excess of dry KBr (Uvasol®, Merck) and thoroughly ground in an agate mortar to a fine homogenous powder.

2.4. Trace analysis

Trace analyses were carried out using a *PlasmaQuad* 3 ICP-MS (VG Elemental). Hundred milligram of each pigment (before and after ball-milling) were dissolved in 50 ml 1.5 M HNO_3 and diluted 4:10. Ti, Cr, Mn, Fe, Co, Ni, Cu, Zn, Mo, Ag, Cd, W and Pb were determined quantitatively (external calibration) whereas concentrations of Mg, Ca, Sr, Ba, Al, Sn, Sb, Zr, Y and La were measured semi-quantitatively. In the latter method, the known concentrations of all calibration solutions are used to construct a calibration curve over the whole mass range for those elements that are not determined by means of external calibration. Sc, Ga, In, Ho and Tl each of 10 ppb were chosen as the internal standard, and preliminary analyses were accomplished to ensure that none of these elements are present in any of the pigments in significant amounts.

2.5. Preparation of pigment coatings

For the determination of lightfastness (details see below), baking finishes that are based on a standard alkyd system were applied. Pigment (6.0 g) (dried at 130 °C for 2 h), 15.0 g lead-free glass beads and 14.0 g baking finish were placed in agate grinding bowls and ground for 1 h.

The pigment lacquers were applied to test sheets, using a 200 μm spiral film applicator (spiral film applicator model 358, Erichsen), and stored in a fume hood for 30 min and another 30 min at 130 °C. The procedure was repeated to obtain a quasi-infinitely thick coating (full shade).

2.6. Illumination experiments

Test sheets were illuminated over a period of 150 min with a 1000 W tungsten halogen lamp (50 cm distance from sample surface) and kept in the dark for 30 min before reflectivity measurements were carried out.

2.7. UV-VIS spectroscopy

Diffuse reflectance spectra were recorded on a double-beam UV-VIS-NIR spectrometer *Lambda* 19 (Perkin–Elmer) equipped with an integrating sphere RSA-PE-19 (Labsphere) in 8/d geometry without inclusion of gloss. For data evaluation, three spectra of each sample were averaged and converted to absolute reflectivity values.

2.8. Quantification of photochromism

In order to describe the degree of color change due to illumination quantitatively, a suitable and well-defined property is needed. The difference in absorption behavior (e.g. change of absorption coefficients) seems to be the parameter of choice, but two facts should be considered. First, deriving accurate absorption properties of strongly absorbing and scattering powders is not straightforward, and second, in the case of pigments, attention is primarily focussed on color sensation, which is restricted to the visible part of the spectrum (380–780 nm) and involves psychological as well as physiological elements. The apparent problem can be solved by means of colorimetry, and many industrial test methods for chromatic and achromatic pigments are based on colorimetric principles. Instead of absorption or transmission measurements, diffuse reflectance spectra are relevant to pigments and provide all information needed to properly describe the strength of the photochromic effect. Though colorimetry is not a standard method in solid-state chemistry, only some fundamental aspects and equations will be given below. For more details and specific test procedures applied in industrial pigment production see, e.g., [17].

The principles of colorimetry are based on the idea of additive color mixing. By choosing three suitable reference colors, it should be possible to produce all colors perceivable by the human nervous system, and the fractions of these references can be taken for a quantitative description of the color in question.[4] Different color spaces have been established, and there is mainly one non-profit organization, the *International Commission on Illumination* (CIE, [18]), which develops and provides standards and procedures in the field of light and lighting.

Basically, three functions are needed that give the fractions of each reference color whose additive mixture matches all spectral colors throughout the visible part of the spectrum. These functions are called CIE color

[4]In fact, this is not really the case, and a unique set of three colors that covers the whole (visible) color space does not exist. The concept of virtual colors must be applied instead (see cited reference).

matching functions ($x(\lambda)$, $y(\lambda)$ and $z(\lambda)$) and are available from 380 to 780 nm in steps of 1 nm. Due to the fact that the three receptors responsible for color perception are not uniformly distributed over the retina, two different sets exist. They define the so-called 2°- and 10°-standard observers for small and large fields of view, respectively. $y(\lambda)$ is somewhat special as it coincides with the spectral luminosity curve of the human eye for photopic vision.

Summing up the color matching functions over the visible range, one obtains color co-ordinates for "white". In order to get co-ordinates for an arbitrary sample, $x(\lambda)$, $y(\lambda)$ and $z(\lambda)$ have to be multiplied by the corresponding reflectance spectrum $\rho(\lambda)$ before summing up. This holds only for illumination with light of constant spectral distribution, a rather hypothetical situation. Normally, weighting with the spectral distribution function $S(\lambda)$ of the light source is required.[5] Several standard illuminants have been defined, e.g., standard illuminant A for incandescent light or D65 for natural daylight at a color temperature of 6504 K.

The following equations summarize the foregoing explanations. Therein, **F** represents the total color stimulus resulting from additive mixing the reference stimuli **X**, **Y** and **Z**. In Eqs. (1) and (2), the quantity m can be regarded as a physical measure for intensity:

$$\mathbf{F} = X \cdot \mathbf{X} + Y \cdot \mathbf{Y} + Z \cdot \mathbf{Z} = m \cdot (x \cdot \mathbf{X} + y \cdot \mathbf{Y} + z \cdot \mathbf{Z}), \tag{1}$$

$$x = \frac{X}{X+Y+Z}, \quad y = \frac{Y}{X+Y+Z}, \quad z = \frac{Z}{X+Y+Z}, \quad m = X + Y + Z, \tag{2}$$

$$\mathbf{F}(\lambda_i) = x(\lambda_i) \cdot \mathbf{X} + y(\lambda_i) \cdot \mathbf{Y} + z(\lambda_i) \cdot \mathbf{Z}, \tag{3}$$

$$\mathbf{F} = K \cdot \sum_{380}^{780} \rho(\lambda_i) \cdot S(\lambda_i) \cdot \mathbf{F}(\lambda_i) \cdot \Delta\lambda,$$

$$\mathbf{F} = K \cdot \sum_{380}^{780} \rho(\lambda_i) \cdot S(\lambda_i) \cdot \{x(\lambda_i) \cdot \mathbf{X} + y(\lambda_i) \cdot \mathbf{Y} + z(\lambda_i) \cdot \mathbf{Z}\} \cdot \Delta\lambda, \tag{4}$$

$$X = K \cdot \sum_{380}^{780} \rho(\lambda_i) \cdot S(\lambda_i) \cdot x(\lambda_i) \cdot \Delta\lambda,$$

$$Y = K \cdot \sum_{380}^{780} \rho(\lambda_i) \cdot S(\lambda_i) \cdot y(\lambda_i) \cdot \Delta\lambda,$$

$$Z = K \cdot \sum_{380}^{780} \rho(\lambda_i) \cdot S(\lambda_i) \cdot z(\lambda_i) \cdot \Delta\lambda,$$

$$K = \frac{100}{\sum_{380}^{780} S(\lambda_i) \cdot y(\lambda_i) \cdot \Delta\lambda}. \tag{5}$$

The tristimulus values X, Y and Z are co-ordinates in a three-dimensional vector space and used to mathematically describe a color with color stimulus **F**. For graphical display, the chromaticity co-ordinates x and y are the preferred quantities. Fig. 2 shows the familiar shoe-sole-shaped CIE chromaticity diagram. The third parameter, which accounts for brightness, is chosen to be Y as it depends on $y(\lambda)$ only. By use of the scaling factor K, Eq. (5), all color co-ordinates are related to an ideal matt-white surface ($\rho(\lambda) = 1$). A beneficial property of the chromaticity diagram is as follows: the color locus of any mixture of two colors lies on a straight line connecting their co-ordinates, the position being determined by the center of gravity principle. It becomes clear that indeed no unique set of three (real) colors exist that allows for all perceivable colors to be produced by additive mixing.

A major disadvantage turns out to be the fact that the CIE system does not constitute a physiologically equidistant color space, i.e., the same distance in different parts of the color space does not agree with the perceived color difference. For pigment testing and quality control, one has to use another set of color co-ordinates, which are calculated from X, Y and Z. The most widely used system is the CIELAB color space shown in Fig. 3. The necessary equations that transform CIE to CIELAB co-ordinates are given by Eqs. (6)–(8), and U, U^*, U_N and $u(\lambda_i)$ have been introduced for the purpose of abbreviation.

Again three parameters are needed for a numerical description of colors: lightness L^*, hue h^*_{ab} and chroma C^*_{ab}. Whereas h^*_{ab} (an angle between 0° and 360°) tells about the kind of color (e.g., red, yellow, green, blue), C^*_{ab} is a measure for saturation. Both are calculated from the values a^* and b^* that constitute the x- and y-axis of the CIELAB color space. The color difference $\Delta E_{ab}{}^*$ is calculated according to Eq. (10).

$$U^* = \begin{cases} \sqrt[3]{\frac{U}{U_N}} & \text{for } U/U_N > 0.008856, \\ 7.787 \cdot \frac{U}{U_N} + 0.138 & \text{for } U/U_N \leqslant 0.008856, \end{cases}$$

where $U \in \{X, Y, Z\}$, (6)

$$U_N = K \cdot \sum_{380}^{780} S(\lambda_i) \cdot u(\lambda_i) \cdot \Delta\lambda_i,$$

where $u(\lambda_i) \in \{x(\lambda_i), y(\lambda_i), z(\lambda_i)\}$, (7)

[5] In case of luminescing materials, care must be taken to account for the additional contribution of emission. A correct instrumental setup requires the monochromator to be placed between sample and detector.

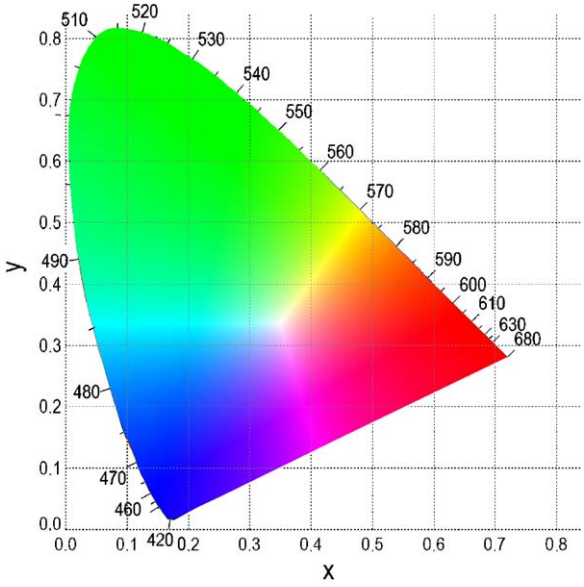

Fig. 2. CIE chromaticity diagram (10°-standard observer). This figure was drawn by means of the program *Chromaticity* (© 1998–2004 Earl F. Glynn II, [19]).

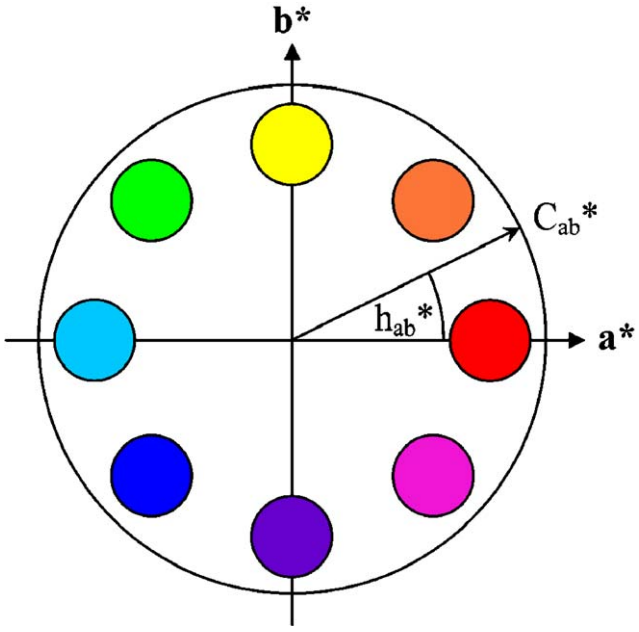

Fig. 3. CIELAB color space—cut through (a^*, b^*)-plane (this figure should only be regarded as a rough approximation for the purpose of illustration; the L^*_{ab}-axis is normal to the drawing plane and ranges from 0 to 100, i.e., from black to white).

$$L^* = 116 \cdot Y^* - 16, \quad a^* = 500 \cdot (X^* - Y^*), \quad b^* = 200 \cdot (Y^* - Z^*), \tag{8}$$

$$h^*_{ab} = \phi + \arctan\frac{|b^*|}{|a^*|}, \quad C^*_{ab} = \sqrt{a^{*2} + b^{*2}}, \tag{9}$$

$$\phi = 0^\circ \text{ for } b^* > 0, a^* > 0, \quad \phi = 90^\circ \text{ for } b^* > 0, a^* < 0,$$
$$\phi = 180^\circ \text{ for } b^* < 0, a^* < 0, \quad \phi = 270^\circ \text{ for } b^* < 0, a^* > 0,$$
$$\Delta E^*_{ab} = \sqrt{\Delta L^{*2} + \Delta a^{*2} + \Delta b^{*2}}. \tag{10}$$

For mechanistic studies of photochromism, optical properties outside the visible range might also be of interest. Therefore, reflectance spectra were recorded up to 1800 nm, and among several possibilities "difference reflectance spectra" (DRS) were chosen to study the diversity in optical behavior of the pigments after illumination. DRS are obtained by subtracting $\rho(\lambda)$ of the illuminated sample from $\rho(\lambda)$ of the sample in its initial state:

$$\Delta\rho(\lambda) = \rho_{\text{initial}}(\lambda) - \rho_{\text{illuminated}}(\lambda). \tag{11}$$

3. Results and discussion

3.1. Phase analysis

In this section, some general aspects of phase purity in relation to different preparation conditions are discussed. It is mandatory to know about the presence of other phases besides monoclinic $BiVO_4$, which is the thermodynamically stable one at standard conditions. This necessity arises because it must be clear whether the photochromic effect is solely caused by the pigment or by any other compound, e.g., V_2O_5, which might form in the course of synthesis and is known for exhibiting photochromism on its own [2]. Thorough inspections of XRD powder patterns only yield information about crystalline impurities, but infra-red spectroscopy will help identifying amorphous compounds.

The phase diagram [13] of the system Bi_2O_3–V_2O_5 shows $Bi_4V_2O_{11}$ and V_2O_5 as neighboring phases, but especially in precipitation reactions meta-stable amorphous or crystalline compounds might occur (e.g., preparation of Zircon-type $BiVO_4$ by precipitation from acidic solutions). At first, we will restrict the discussion to pigments synthesized by wet-chemical routes. Today these methods are the only important ones in industrial pigment production of $BiVO_4$ yielding better color properties and facilitating easier processing of raw products.

Potential factors of influence on phase purity can be confined to the choice of the Bi:V ratio, the pH value before and pH control while heating the suspension. Of course, additives can play an important role. In some reactions, NH_4NO_3 was added for passive pH regulation and for doping pigments small amounts of suitable compounds were dissolved in either the bismuth or vanadate solution. Only in some cases were larger

dopant concentrations chosen, but the influence on pH evolution can be significant (see below).

Figs. 4 and 5 show a series of powder patterns obtained after thermal treatment. Table 1 includes the pigments in question as well as the corresponding parameters of synthesis and impurity phases found in the thermally treated products.

The occurrence of impurity phases turns out to be characteristic under the chosen reaction conditions if a stoichiometric Bi:V ratio is applied and the pH value of the suspension is allowed to develop without constraint. After annealing at 500 °C, the powder pattern of BV-116 shows the largest amount of an additional phase labelled *X*. Unfortunately, it has not been possible so far to identify the origin of these peaks. They vanish after heating to 750 °C, and new ones appear that can be attributed to $Bi_4V_2O_{11}$ (BV21). Assuming that no significant portion of amorphous material is present if annealing is carried out at 500 °C, the phase *X* must also contain more bismuth than vanadium. For BV-116 approximately 3.0% $Bi_4V_2O_{11}$ were determined by Rietveld analysis, which corresponds to an overall Bi:V ratio of 1.018:1. Increasing the V content or reducing the final pH value leads to decreasing amounts of *X* or $Bi_4V_2O_{11}$. This can be achieved by lowering the initial pH or by controlling the development of pH in a passive (adding a suitable buffer, e.g., NH_4NO_3) or active manner (continuously adding HNO_3). The rise in pH on heating the suspension is probably due to a transformation of some kind of basic bismuth vanadate (Bi tends to form basic nitrates, carbonates, halides) to crystalline monoclinic $BiVO_4$. Doping with 5 mole-% Ca or Sr, which both do not form basic compounds, leads to a smaller increase of pH (4.8 → max. 7.5; 3.8 → max. 5.0), and in all cases single phase products were obtained. Nevertheless, it is somewhat problematic to generalize these findings, and different reaction conditions (temperature, heating period, concentration of Bi and V solution) can lead to slightly differing results. Some interesting details about the influence of synthesis conditions were reported by Wood and Glasser [11] who studied the preparation of $BiVO_4$ by precipitation at lower pH values (final pH ~2 or below), which results in considerable amounts of the Zircon-type modification as primary product. The interesting point with respect to our study is the fact that they also found slight excesses of bismuth in thermally treated raw-products. As a possible explanation the substitution of VO_4^{3-} by OH^- or NO_3^- was suggested.

Some final remarks are dedicated to amorphous phases, where the focus is directed to the possibility of V_2O_5 formation. Any large excess of V_2O_5 is easily removed by carefully washing the raw product. Since powder diffraction requires crystalline material,

Table 1
Dependency of phase purity on synthesis parameters (wet-chemical method)

Sample name	Bi:V ratio	ΔpH	Annealing	Phases[a]
BV-116	1 : 1	4.5 → 9.6	2 h 500 °C	BV, *X*
			2 h 750 °C	BV, BV21
BV-123	1 : 1	3.8 → 8.5	2 h 500 °C	BV, *X*
			2 h 750 °C	BV, BV21
BV-124	1 : 1.01	3.8 → 8.8	2 h 500 °C	BV, *X*
			2 h 750 °C	BV, BV21
BV-132	1 : 1.02	3.8 → 8.4	2 h 500 °C	BV
			2 h 750 °C	BV
BV-143	1 : 1.01	3.8 → 4.9 (NH_4^+-buffer)	2 h 500 °C	BV
BV-149	1 : 1.012	3.8 → 4.8 (pH control)	2 h 500 °C + 0.5 h 620 °C	BV

[a]BV = monoclinic $BiVO_4$, BV21 = $Bi_4V_2O_{11}$, *X* = unknown impurity phase.

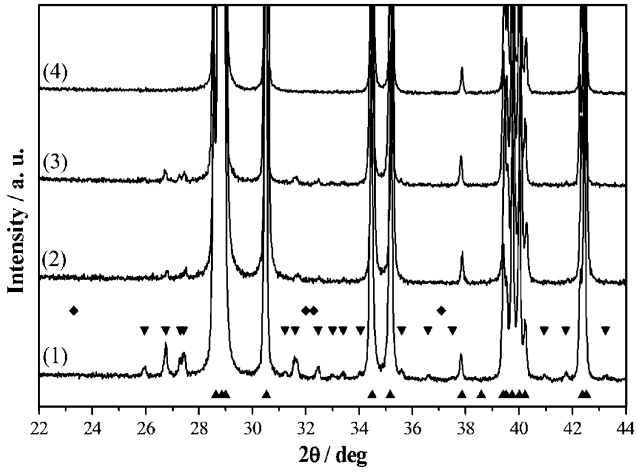

Fig. 4. Powder diffraction diagrams of different pigments annealed at 500 °C for 2 h: (1) BV-116, (2) BV-123, (3) BV-124, (4) BV-132 (▲ monoclinic $BiVO_4$ ▼ impurity phase *X* ◆ $Bi_4V_2O_{11}$).

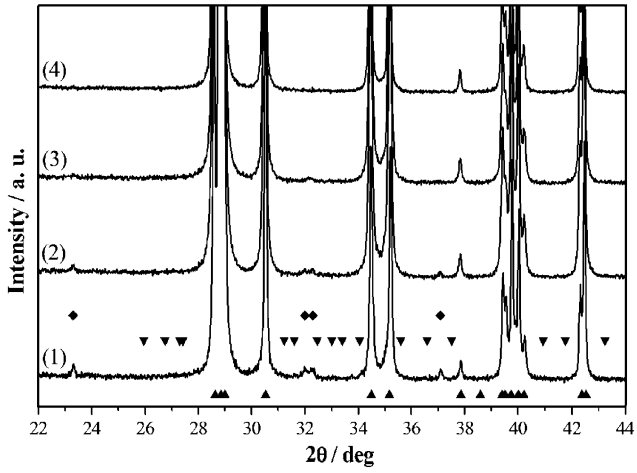

Fig. 5. Powder diffraction diagrams of different pigments annealed at 750 °C for 2 h: (1) BV-116, (2) BV-123, (3) BV-124, (4) BV-132 (▲ monoclinic $BiVO_4$ ▼ impurity phase *X* ◆ $Bi_4V_2O_{11}$).

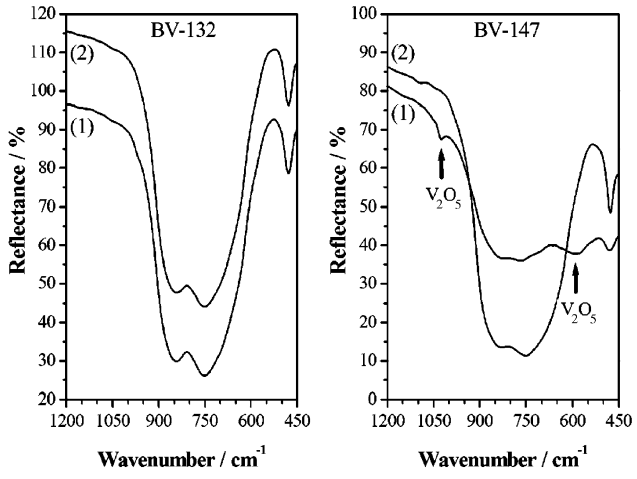

Fig. 6. Infra-red spectra of BV-132 (2 h 500 °C) and BV-147 (solid-state reaction, 3 × 10 h 650 °C): (1) without ball-milling (2) after ball-milling, spectrum of BV-132 shifted by +20%.

infra-red spectroscopy is an important alternative. Fig. 6 shows infra-red spectra in the range between 1200 and 450 cm^{-1} for two pigments, namely BV-132 and BV-147, before and after ball-milling. The latter was synthesised by solid-state reaction starting from a mixture of Bi_2O_3 and V_2O_5, which was annealed in three successive steps. Evidence for the existence of V_2O_5 is found only in the case of pigments prepared by solid-state reaction. All compounds synthesized by wet-chemical routes turn out to be free of V_2O_5. Surprisingly, the same holds true for the former group of pigments after ball-milling. This indicates re-crystallisation while removing the water by vaporization or completion of the reaction by mechanical force. According to XRD, all pigments obtained by solid-state synthesis are single-phase compounds regardless of the kind of mechanical after-treatment. These findings stress the usefulness of infra-red spectroscopy to complement powder diffraction in qualitative phase analysis.

3.2. Trace analysis

Perovskites are prime examples for compounds where impurities or dopants are the cause of photochromic effects. Thus, it becomes evident that detailed information about the content of trace elements is necessary in studies of potential reasons for the photochromism of bismuth vanadate. Regarding phase purity, it seems highly desirable that pigments are either single phase or contain only small amounts of compounds other than $BiVO_4$. The latter is important since element analysis only provides average concentrations but cannot identify the proper sources of impurities. For all pigments under investigation, the quantities of phase *X*, if present at all, are significantly lower than for BV-116.

Because of the large amounts of experimental data, it is somewhat difficult to keep track of the more important facts, and some of the elements mentioned in the experimental section will be omitted from the following discussion. Only those elements that seem to be relevant with regard to photochromism, i.e., predominantly transition metal elements, will be included in the discussion.

The bar charts in Figs. 7 and 8 show concentrations (μg element per g pigment) of selected elements for pigments after ball-milling. Compared to the corresponding unground samples, only small increases were found in most cases, except for earth alkaline elements, but these do not enhance the photochromic effect of $BiVO_4$ as will become clear later.

Fe, Ni, Mo, Ag and W are among the elements included in Figs. 7 and 8, and all of them have been

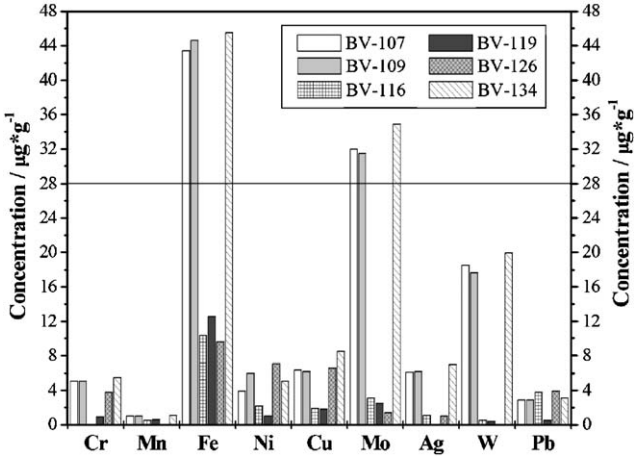

Fig. 7. Concentrations of trace elements for selected pigments (only values ⩾0.3 ppm are given; the horizontal line indicates the upper limit in Fig. 8 for easier comparison).

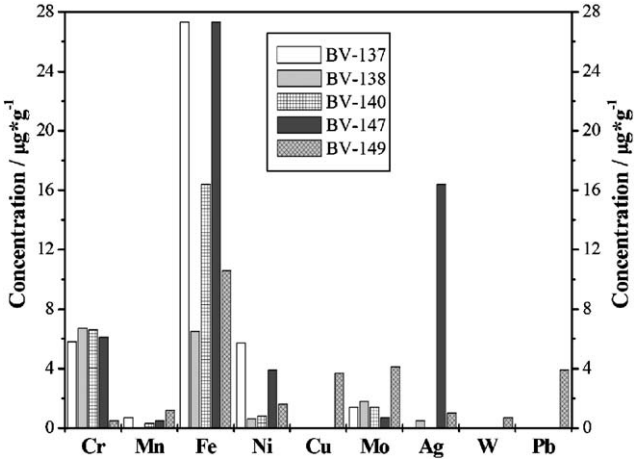

Fig. 8. Concentrations of trace elements for selected pigments (only values ⩾0.3 ppm are given).

encountered in other photochromic materials (see references cited in the Introduction section). Co, which can also cause color changes in perovskites on illumination [7], is left out as only very small amounts (< 0.3 ppm) that did not vary significantly from sample to sample were measured in all cases. One pigment, viz. BV-138, deserves a short remark. Instead of following the usual wet-chemical precipitation route, BV-138 was prepared by stirring a suspension of Bi_2O_3 and V_2O_5 in 1 M HNO_3 at 25 °C for 5 days. Prior to filtering and washing, the pigment was kept for another 5 days at room temperature.

The largest differences in concentrations are found for Fe, Mo, Ag and W while impurity levels of Mn are almost negligible. Pb contents generally lie below 4 ppm and in some cases even below the detection limit. BV-137 and BV-147 were synthesized by solid-state reaction, but except for Fe no clear-cut distinction to other samples can be drawn (the relatively high concentration of Ag in BV-147 is caused by a contamination of unknown origin). The special preparation method mentioned above is the reason why BV-138 contains overall fewer impurities than any other compound. Acidic conditions inhibit adsorption of cations on the particles surface, and thus occlusion hardly takes place.

Considering the bar chart in Fig. 9, impurity distributions can be traced back to the starting compounds (see Table 1 for assignments between pigments and educts). Slight variations are due to differences in the purity of chemicals (nitric acid, sodium hydroxide, de-ionized water) and other contaminations during the whole process of after-treatment.

3.3. Illumination experiments with pigment coatings

In this section, results of illumination experiments are discussed that were obtained from pigment coatings (full shade) applied on suitable test sheets. Data evaluation is based on colorimetry as described in Section 2. The most important point is to ensure sample illumination under reproducible conditions. In principle, the lightfastness of pigments in natural daylight is of interest, but due to lacking in constancy of irradiance, stability tests under "natural conditions" are usually restricted to long-term inspections of weatherfastness. Unfortunately, there is no light source recommended by the CIE to simulate natural daylight. It is quite common to utilize xenon lamps while the use of halogen lamps is becoming more and more out-dated. Nevertheless, lightfastness or the magnitude of photochromism can be analyzed by illuminating with halogen light and calculating ΔE_{ab}^*-values from the color co-ordinates of the initial and final state.

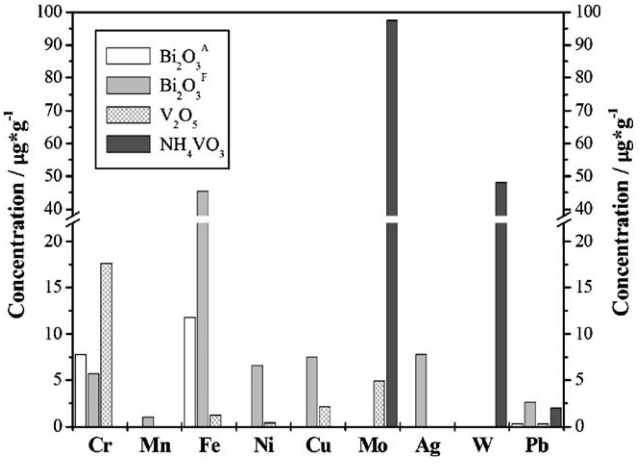

Fig. 9. Concentrations of trace elements for different educts (only values ⩾0.3 ppm are given).

Table 2 includes information like parameters of synthesis, phase analysis and ΔE_{ab}^*-values for those pigments that have already been introduced in the previous subsection. The range of ΔE_{ab}^* extends from 0.9 (color change hardly visible) to 5.6 (strong photochromic effect).[6] The existence of correlations between ΔE_{ab}^* and the choice of educts or the thermal treatment are of major interest, but one should also keep in mind that the duration of ball-milling is determined by the annealing temperature.

The first striking fact is the circumstance that weak as well as intense photochromism is found for pigments irrespective of compound X being present or not. Obviously, small quantities of this impurity phase do not exert any influence on the photochromic properties. Recalling that BV-116 contains the largest amounts of X and ΔE_{ab}^* is 1.7 only (in the case of annealing for 2 h at 500 °C) no additional complication resulting from X will be encountered for any other samples.

The next point to be mentioned is the observation of increasing ΔE_{ab}^*-values if annealing is carried out under more rigorous conditions, as can be exemplified by BV-116, BV-140 and BV-149. Surprisingly, solid-state reactions do not always yield strongly photochromic pigments (compare BV-109 with BV-137 and BV-147).

At this stage it appears useful to differentiate between pigments prepared by wet-chemical and solid-state methods. In case of the former, the outcome of illumination experiments seems to significantly depend on the choice of educts. BV-107 as well as BV-134 exhibit strong photochromism, and by replacing the Bi or V solution with solutions prepared from solid $Bi_2O_3^A$ or V_2O_5 improvements in lightfastness result, finally ending in BV-140 being the pigment with the lowest ΔE_{ab}^* of all samples (consider the following series: BV-116/149 → BV-119 → BV-126 → BV-140). The starting compounds directly affect the maximum levels of trace impurities, and Fig. 10 shows a comparison between

[6] Comparing different pigments, differences in ΔE_{ab}^* of about 0.4 can be considered significant.

Table 2
ΔE^*_{ab}-values (coatings), synthesis parameters and phase analysis for undoped pigments

Sample	Educts[a]	Bi : V	ΔpH	Annealing	XRD[b]	ΔE^*_{ab}
BV-107	$Bi_2O_3^F/NH_4VO_3$	1 : 1	4.5→4.8	2 h 500 °C	BV, *X*	5.3
BV-109	$Bi_2O_3^F/NH_4VO_3$	1 : 1	SSR[c]	3 × 10 h 650 °C	BV	2.5
BV-116	Bi sol./V sol.	1 : 1	4.5→9.6	2 h 500 °C	BV, *X*	1.7
				2 h 750 °C	BV, BV21	3.4
BV-119	$Bi_2O_3^A/V$ sol.	1 : 1	4.5→9.7	2 h 500 °C	BV, *X*	1.4
BV-126	Bi sol./V_2O_5	1 : 1	3.8→8.5	2 h 500 °C	BV, *X*	1.3
BV-134	$Bi_2O_3^F/NH_4VO_3$	1 : 1.01	4.5→5.9	2 h 500 °C	BV, *X*	4.5
BV-137	$Bi_2O_3^A/V_2O_5$	1 : 1.01	SSR[c]	3 × 10 h 650 °C	BV	5.6
BV-138	$Bi_2O_3^A/V_2O_5$	1 : 1.01	—[d]	2 h 500 °C	BV	2.6
BV-140	$Bi_2O_3^A/V_2O_5$	1 : 1.01	3.8→8.8	2 h 500 °C	BV, *X*	0.9
				2 h 500 °C + 0.5 h 620 °C	BV, *X*	2.1
				3 × 10 h 650 °C	BV, *X*	3.0
BV-147	$Bi_2O_3^A/V_2O_5$	1 : 1.01	SSR[c]	3 × 10 h 650 °C	BV	5.4
BV-149	Bi sol./V sol.	1 : 1.01	3.8→4.8	2 h 500 °C	BV, (*X*)	2.2
				2 h 500 °C + 0.5 h 620 °C	BV	2.6

[a]Solutions of Bi and V were provided by BASF; $Bi_2O_3^F$: Fluka; $Bi_2O_3^A$: Alfa.
[b]BV = monoclinic $BiVO_4$, BV21 = $Bi_4V_2O_{11}$, *X* = unknown impurity phase.
[c]Solid-state reaction.
[d]Stirring in HNO_3 (see Section 2).

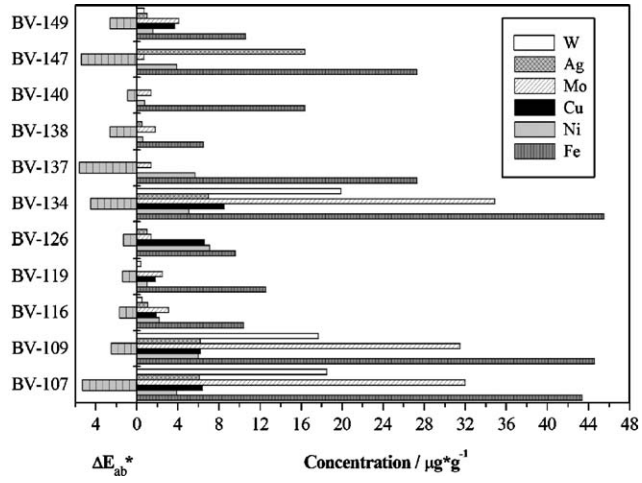

Fig. 10. Comparison between levels of trace elements and ΔE_{ab}^*-values (only concentrations ⩾0.3 ppm are given).

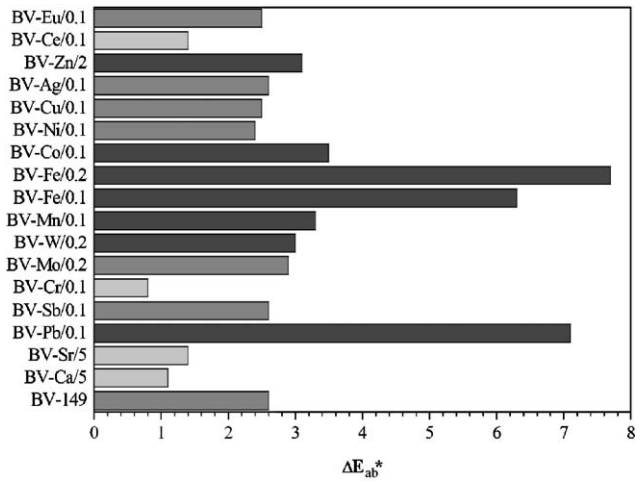

Fig. 11. ΔE_{ab}^*-values for coatings of doped pigments compared to BV-149 (reference pigment) (the number after each element corresponds to the nominal concentration in mole-%; different shadings indicate differences in ΔE_{ab}^* of at least 0.3 relative to BV-149).

ΔE_{ab}^*-values and concentrations of selected elements (Cr, Mn and Pb have been left out).

Obviously, Cu and Ni cannot play an important role as is quickly understood by comparing, e.g., BV-107 with BV-126. On the other hand, the remaining elements need a closer examination. Those pigments exhibiting intense photochromism contain larger amounts of Mo and W, but the latter does not account for the differing properties of BV-138 and BV-140. In the case of Ag, similar arguments apply to the behavior of BV-126 and BV-138 (higher ΔE_{ab}^*, lower Ag concentration). Finally, the concentrations of Fe can at first sight not satisfactorily account for the weak photochromism of BV-140, but BV-107 and BV-134 are pigments comparatively rich in Fe. The preliminary conclusion is that there is no "perfect" correlation between Fe levels and ΔE_{ab}^* or secondary factors must be considered to account for the partly ambiguous findings. Nevertheless, the potential influence of Mo, W, Ag and Fe suggests further investigations, and doping "pure" $BiVO_4$ is a useful start. The precipitation of impurity phases must be avoided but, anyway, one should operate at doping levels that are in accordance with the trace levels determined, e.g., for BV-107.

The bar chart in Fig. 11 includes a compilation of ΔE_{ab}^*-values obtained for doped pigments that were synthesized in the same way as BV-149 (reference compound). Usually, concentrations of 0.1 mole-% were

chosen to allow for easy handling without exceeding reasonable doping levels. Indeed, not only doping with Fe causes strong photochromic effects but also doping with Pb. The latter finding could not be expected as all pigments under study did not show any noteworthy variation in Pb content but low concentrations, instead. In contrast to Fe, neither Mo nor W nor Ag can be made responsible for the low lightfastness of BV-107 or BV-134. The results also confirm that Cu and Ni are not important as was inferred from trace analysis.

Another interesting aspect is the influence of Ca and Sr where higher concentrations were chosen (as is usually done in the case of commercially available $BiVO_4$ pigments). Lower values of ΔE_{ab}^* are found, and, except for Cr and Ce, these are the only dopants that turn out to notably improve lightfastness. Despite their low concentrations, Cr and Ce already cause significant color changes in the non-illuminated state due to absorption at energies below the band gap of $BiVO_4$ (approx. 2.4 eV as was derived from plots of absorbance $A = \log(1/\rho(\lambda))$ of pure pigment powders). This is the main reason why illumination-induced absorption does not reduce the reflectance as strongly in this case as it would do if starting from higher initial values of reflectivity.[7]

Fig. 12 shows reflectance spectra of doped pigments and BV-149 before illumination. The spectra of 0.1% Fe-doped and 0.1% Pb-doped $BiVO_4$ have been shifted by +5% and +10% reflectance, respectively. In contrast to Ce and Cr, neither Fe nor Pb cause noticeable changes in the spectra if compared to BV-149. This can be explained by a lack of deep defect states or a negligible increase in absorption in these cases due to the combined effects of low transition probabilities and low concentrations. The latter arguments seem reasonable for Fe only as this dopant was found to substitute for V and exists in the +III high-spin oxidation state [16]. The corresponding Fe3d→Fe3d transitions are spin-forbidden and Fe3d→CB transitions can approximately be described as Fe3d→V3d transitions,[8] which (recalling the Scheelite-type structure of $BiVO_4$ where isolated $[VO_4]$ tetrahedra occur) will exhibit low transition probabilities as well.

As mentioned earlier, difference reflectance spectra (DRS) are an appropriate means to qualitatively characterize differing optical properties of pigments after illumination. Fig. 13 includes DRS for BV-147, BV-149, BV-Fe/0.1 and BV-Pb/0.1. Apparently, three types of spectra can be distinguished. The DRS of BV-147 and BV-149 are quite similar and show one single peak that falls off slowly towards longer wavelengths.

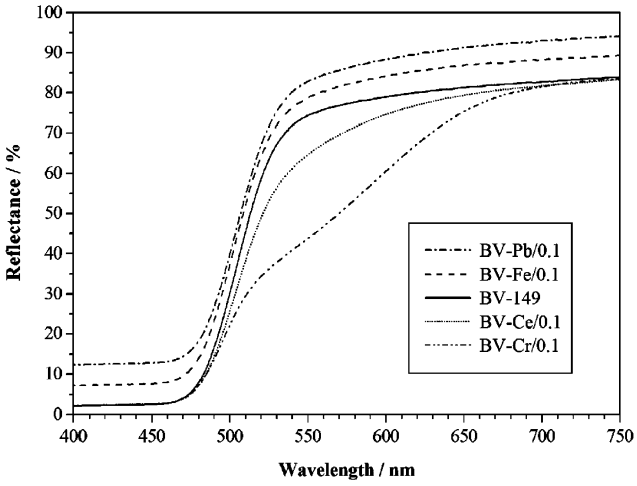

Fig. 12. Reflectance spectra of BV-Fe/0.1, BV-Pb/0.1, BV-Cr/0.1, BV-Ce/0.1 and BV-149 (pigment coatings, non-illuminated; see text).

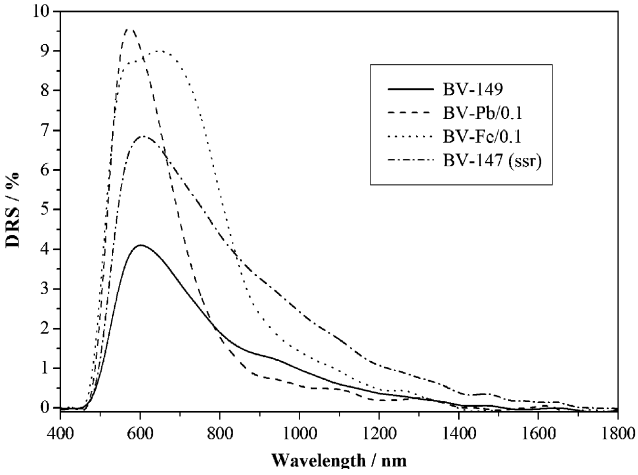

Fig. 13. Difference reflectance spectra (DRS) of BV-149, BV-Fe/0.1, BV-Pb/0.1 and BV-147 (pigment coatings; for explanation of DRS see text).

On the other hand, the DRS of BV-Pb/0.1 exhibits a more intense maximum but falls off steeply. The third type of DRS is found for BV-Fe/0.1 where a "double-band structure" appears as characteristic feature.

Indeed, the DRS of many other pigments can be assigned to one of these three types of spectra. It is possible to distinguish at least three different mechanisms of photochromism for $BiVO_4$ and to classify them according to their DRS. Difficulties are expected to arise if only medium or weak photochromic effects are observed ($\Delta E_{ab}^* < 2.5$) because the characteristic features of the corresponding DRS might not be pronounced enough.

Unfortunately, there is no simple relation between DRS and absorption coefficients. It does not make sense to fit a series of Gaussian peaks (or other appropriate functions) and assign energy values. First of all, any

[7]This statement can be verified by recalling the relation between reflectivity and the Kubelka–Munk function [20].

[8]According to band structure calculations (LMTO–ASA, [21]) the bottom of the conduction band is primarily V3d in character.

change in absorption will result in variations of refractive index (anomalous dispersion) and, hence, variations in scattering coefficients. On the other hand, structure in absorption peaks might arise as a consequence of band structure, which determines the number of final states in donor→CB (or the number of initial states in VB→acceptor transitions) as well as transition probabilities. Therefore, it seems reasonable to use DRS primarily as an indicator for different mechanisms of photochromism. Nevertheless, some qualitative aspects can be discussed. The DRS in Fig. 13 indicate different threshold energies to be exceeded in absorption processes. Obviously, illumination results in formation of deep defect states (1550 nm corresponds to 0.8 eV), but for BV-Pb/0.1 a higher energy is needed than for BV-Fe/0.1 and BV-147.

The drastic increase in ΔE_{ab}^{*} is a clear indication for the central role of the corresponding dopants in the mechanisms of photochromism. Especially Fe is known for its diversity in oxidation states, and $SrTiO_3$:Fe is a good example for photochemically induced formation of Fe^{IV} metastable states [7]. In $BiVO_4$, Fe^{IV} becomes available by either hole-trapping or direct excitation. The change in oxidation state provides new optical transitions, which are particularly intense if they are of the charge-transfer type.

For pigments exhibiting DRS like BV-149 and BV-147 (where concentrations of Fe or Pb are significantly lower), a change in oxidation state of V itself must be considered. In this case, photochromism could be described as an intrinsic property of the material. The baking finish used to prepare the coatings contains dicarboxylic acids, poly alcohols and an organic solvent.[9] Because of incomplete esterification during baking, free carboxyl groups (donors of protons) and hydroxyl groups (reducing agent) remain and open up photochemical reactions, e.g., the reduction of V^{V} to V^{IV}. The latter species introduce donor states below the conduction band and finally pass into a donor band if sufficient defects are formed. For more details, one has to resort to other spectroscopic techniques like electron-paramagnetic resonance.

The final remark is left to pigment BV-109, which was synthesized by solid-state reaction starting from the same compounds used for BV-107 and BV-134. The latter two reveal strong photochromism whereas for BV-109 only a moderate ΔE_{ab}^{*}-value is observed. The main difference between these samples is due to thermal and mechanical treatment. Referring back to the ideas given above, two fundamentally different situations arise. On the one hand, interactions between pigment particles and the surrounding lacquer are involved leading to photochemical reduction. The extent of reduction is primarily determined by the contact surface, i.e., the specific surface of the pigment in question. In contrast, the formation of Fe^{IV} does not require reactions with lacquer components, which indeed tend to suppress any kind of oxidation process. Thus, different conditions (pigment surface, Fe concentration, red-ox properties of the surrounding medium) will result in different photochromism mechanisms as well as different types of DRS.

[9]In fact, the solvent is a complex mixture of organic compounds with varying volatilities.

4. Conclusions

In the preceding sections, we have presented an approach that is widely used in industrial color testing to study the photochromic properties of $BiVO_4$ pigments but hardly known among solid-state chemists. Therein, colorimetry is of central importance and provides a mathematical procedure to quantitatively describe the extent of color change (ΔE_{ab}^{*}-values) due to illumination of pigment coatings.

Two different routes were chosen to prepare $BiVO_4$ pigments. Today, wet-chemical precipitation methods have superseded solid-state reactions in industrial pigment production. However, in studies of photochromism the results derived from both ''types'' of pigments can complement each other.

In order to obtain unambiguous results, the dependency of phase purity on synthesis conditions was investigated. In precipitation methods, small excesses of Vanadium and controlling the evolution of pH during the heating period by continuously adding HNO_3 give rise to single-phase pigments. The absence of V_2O_5 was confirmed by DRIFT measurements of powder samples. However, small amounts of other impurity phases did not cause any significant increase in photochromism.

As the choice of educts was found to strongly affect lightfastness, comprehensive trace analyses were carried out to reveal correlations between impurity levels and ΔE_{ab}^{*}-values. By means of doping experiments, such correlations were proven to exist for Fe. The same holds true in the case of Pb, which accounts for strong photochromic effects if present in considerable amounts.

Some of the results obtained from pigments prepared by solid-state reaction seem to be in conflict with these findings, and additional effects that result from pigment lacquer interactions can only be assumed at this point. Indeed, it will be shown in the second part of this paper that differences in thermal and mechanical treatment result in different specific surfaces of the pigment samples and, therefore, different reactivities with the surrounding media.

Besides the extent of photochromism, given by the color difference ΔE_{ab}^{*}, valuable information is available from difference reflectance spectra. It is possible to differentiate several mechanisms of photochromism according to the shape of the DRS, and in many cases

pigments can be assigned to one of three mechanism types unambiguously. Although absorption coefficients cannot be extracted, the DRS suggest that deep defect levels appear on illumination and are responsible for the observed changes in color from yellow to green. These are believed to result from photochemically induced redox reactions in which, e.g., Fe^{II}, Fe^{IV} or V^{IV} are formed. Similar effects might apply for the "Pb-type" mechanism as well, but more information is still needed in this case.

Acknowledgments

We gratefully acknowledge the substantial support of BASF Ludwigshafen and the helpful discussion with Dr. N. Mronga and Dr. O. Seeger.

References

[1] S.I. Stepanov, Rep. Prog. Phys. 57 (1994) 39.
[2] A. Gavrilyuk, Proc. SPIE 2968 (1997) 195.
[3] U. Tritthart, A. Gavrilyuk, W. Gey, Solid State Commun. 105 (1998) 653.
[4] C. Bechinger, G. Oefinger, S. Herminghaus, P. Leiderer, J. Appl. Phys. 74 (1993) 4527.
[5] M.-H. Huang, J.-Y. Xia, Y.-M. Xi, C.-X. Ding, J. Eur. Ceram. Soc. 17 (1997) 1761.
[6] P. Koidl, K.W. Blazey, W. Berlinger, K.A. Müller, Phys. Rev. B 14 (1976) 2703.
[7] B.W. Faughnan, Phys. Rev. B 4 (1971) 3623.
[8] T.M. Bochakova, M.D. Volnyanskii, D.M. Volnyanskii, V.S. Shchetinkin, Phys. Solid State 45 (2003) 244.
[9] D. Caurant, D. Gourier, M. Prassas, J. Appl. Phys. 71 (1992) 1081.
[10] D. Caurant, D. Gourier, D. Vivien, M. Prassas, J. Appl. Phys. 73 (1993) 1657.
[11] P. Wood, F.P. Glasser, Ceram. Int. 30 (2004) 875.
[12] K. Hirota, G. Komatsu, M. Yamashita, H. Takemura, O. Yamaguchi, Mater. Res. Bull. 27 (1992) 823.
[13] Y.N. Blinovskov, A.A. Fotiev, Russ. J. Inorg. Chem. 32 (1987) 254.
[14] Y.F. Kargin, V.Y. Voevodskii, Russ. J. Inorg. Chem. 42 (1997) 1413.
[15] T.H. Yeom, S.H. Choh, K.J. Song, M.S. Jang, J. Phys.: Condens. Matter 6 (1994) 383.
[16] T.H. Yeom, S.H. Choh, M.L. Du, M.S. Jang, Phys. Rev. B 53 (1996) 3415.
[17] H.G. Völz, Industrial Color Testing. Fundamentals and Techniques, VCH, Weinheim, 1995.
[18] http://www.cie.co.at.
[19] http://www.efg2.com/Lab.
[20] G. Kortüm, Reflectance Spectroscopy: Principles, Methods, Applications, Springer, Berlin, 1969.
[21] S.M. Schlitter, Farbgebungsprozesse in kristallinen Chromat- und Vanadatpigmenten. Theoretische und experimentelle Aspekte der optischen Absorption, Logos, Berlin, 1998.